Metal-Insulator Transitions in Pure and Doped V_2O_3

D. B. McWhan, A. Menth*, J. P. Remeika, W. F. Brinkman, and T. M. Rice
Bell Telephone Laboratories, Murray Hill, New Jersey 07974
(Received 31 January 1972)

The addition of Ti^{3+} and Mg^{2+} to V_2O_3 leads to the suppression of the antiferromagnetic insulating phase; whereas the addition of Ti^{4+}, Zr^{4+}, and Fe^{3+} results in a first-order transition from a metallic to an insulating state. The effect of impurity ions is discussed in terms of the changes they cause in the bandwidth in analogy with the effect of pressure. The Hall coefficient of metallic V_2O_3 at 4.2 °K and 20 kbar is $R_H = +(3.5 \pm 0.4) \times 10^{-4}$ cm^3/C which is close to the value measured at 150 °K and 1 atm. The residual resistivity of metallic V_2O_3 is strongly impurity dependent (140 $\mu\Omega$ cm/at.% Cr and 35 $\mu\Omega$ cm/at.% Ti). These results are not completely consistent with current theories for the metal-insulator transition in V_2O_3 but the best available model still seems to involve a localized-to-nonlocalized transition within the *d* band primarily involving orbitals in the basal plane.

I. INTRODUCTION

Vanadium sesquioxide has a sharp first-order transition from an antiferromagnetic-insulating phase to a metallic phase at 150–162 °K and a region of continuous change back to an insulating state around 500–550 °K. Experiments on the mixed-oxide system $(V_{1-x}Cr_x)_2O_3$ using both temperature and pressure as variables have shown that the two temperature-induced changes are related and that they are part of a more general phase diagram.[1-3] This diagram, which is illustrated in Fig. 1, has three clearly defined regions; metal (M), insulator (I), and antiferromagnetic insulator (AF). It has been argued that the available experimental results are consistent with a transition from a highly correlated metallic phase to a phase which is localized but has polar fluctuations.[1,4] This type of transition as a function of pressure was originally proposed by Mott.[5,6]

The generalized phase diagram shown in Fig. 1 shows that there is an empirical scaling of the addition of Cr^{3+} and a negative pressure. The scaling also appears to hold for the addition of Ti^{3+} and a positive pressure. In an attempt to understand the origin of this correlation a series of doping experiments has been carried out with Ti, Zr, Mg, and Fe. The preparation and characterization of the different samples are described in Sec. II. In Sec. III the physical properties of each system are summarized and in Sec. IV these results are related to the current theory for the metal-insulator transition in V_2O_3.

It is clear that the metal-insulator transition represents a boundary between sesquioxides which are good insulators and those which are metallic, i.e., it is a Mott-type transition. However, a detailed understanding of the transition requires as a minimum the parameters of a paramagnetic band-structure calculation and some understanding of how these parameters change with volume. At present, we have only qualitative speculations as to the nature of the band structure.

Even without this information one can make several predictions for the properties of the metallic state near the transition due to the large local spin fluctuations. With these predictions in mind we have made a series of measurements of the transport properties of the metallic state. These are reported in Sec. V. The Hall coefficient in pure V_2O_3 was measured at liquid-helium temperatures above the critical pressure necessary to suppress the antiferromagnetic phase. Also, the residual resistivity and the coefficient of the T^2 term as a

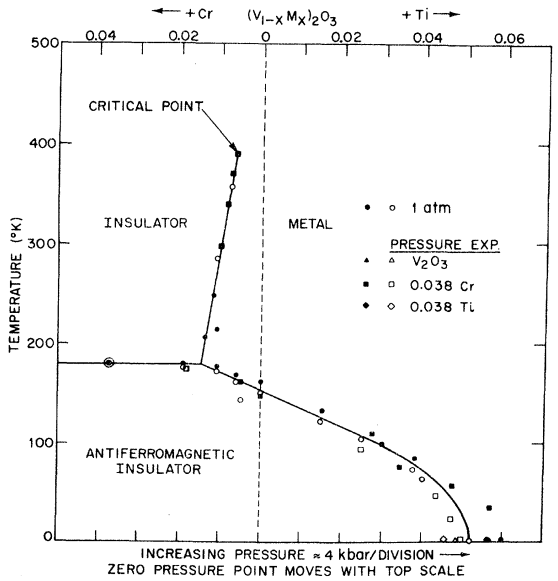

FIG. 1. Generalized phase diagram for the metal-insulator transition in V_2O_3 as a function of doping with Cr or Ti and as a function of pressure (after Ref. 3). The closed and open symbols are for increasing and decreasing pressure or temperature. The metal-insulator boundary terminates at a critical point which is temperature and pressure dependent.

function of doping were measured. These results are discussed in terms of current speculations on the nature of the metallic state of V_2O_3 in Sec. VI. It is concluded that none of the current theories is completely consistent with the available experimental results.

II. PREPARATION AND CHARACTERIZATION OF DOPED V_2O_3 SAMPLES

The methods used to grow crystals of V_2O_3 and also to make ceramic samples have been decribed.[2,7] The crystals are grown in molten KF by reduction of V_2O_5 with VN. It has been found that the reproducibility and quality of the crystals is substantially improved if the KF is premelted at 1150 °C for 2 h prior to use in order to remove any traces of water. Increasing the time of growth to 120 h apparently results in dissolution and regrowth leading to a crystal 1 cm in the largest dimension and with much less occluded VN. As in the V_2O_3–Cr_2O_3 system an appropriate amount of the oxide of the dopant is added to the starting mixture. The actual concentration of the dopant in the crystals is then measured by emission-spectrographic techniques. A few representative samples are listed in Table I.

The conditions used to prepare the ceramic samples are also shown in Table I.[7] The uniformity of the sample is greatly dependent on the care taken in preparing as homogeneous as possible a starting

TABLE I. Characterization of doped vanadium sesquioxide samples.

No.	Concentration	Synthesis	Analysis[e]	Lattice parameters Metal a(Å)	Metal c(Å)	Insulator a(Å)	Insulator c(Å)	Transition Temperatures M-AF I-AF (°K)	M-I(°K)
			Single-crystal samples						
1	0	900 °C, 120 h	M >>> VN	4.951[f]	14.003			150–162[g]	
2	Ti 0.015[a]	TiO_2, 950 °C, 72 h[c]	M >>> V_3O_5	4.957	13.997			124–134[g]	
3	Ti 0.025	TiO_2, 975 °C, 336 h	M ≫ VN	4.962	13.997			104	
4	Ti 0.038	TiO_2, 875 °C, 102 h	M ≫ V_3O_5	4.967	13.994			74–83[g]	None < 1000[g]
5	Ti 0.040	TiO_2, 975 °C, 336 h	M > VN	4.968	13.994			63	None < 650[h]
6	Ti 0.049	TiO_2, 950 °C, 168 h	M ≫ VN					31	
7	Ti 0.051	TiO_2, 930 °C, 275 h	M ≫ VN	4.967	13.995			NONE	
8	Ti 0.081	TiO_2, 950 °C, 336 h	M	4.973	13.993			NONE	
9	Zr 0.001	ZrO_2, 1000 °C, 72 h	M ≫ VN						
10	Zr 0.002	ZrO_2, 950 °C, 72 h	M ≫ VN	4.951	14.000			150–162[g]	
11	Zr 0.003	ZrO_2, 950 °C, 72 h	M ≫ VN	4.957	14.000			150–164[g]	340–400[g]
12	Zr 0.007	ZrO_2, 950 °C, 72 h	M, I ≫ VN	4.960	14.008	5.003	13.952		320–370[h]
13	Zr 0.013	ZrO_2, 950 °C, 72 h	M, I ≫ VN	4.961	14.006	5.004	13.925		260–400[h]
			Ceramic samples						
14	1% TiO_2[b]	1000 °C, 16 h[d]	M ≫ I	4.954	13.999				
15	5% TiO_2	1000 °C, 16 h	M < I	4.956	13.991	4.997	13.925		
16	20% TiO_2	1000 °C, 16 h	M > I ≫ V_3O_5	4.960	13.987	4.993	13.916	150 – 160[h]	< 373[j]
17	2% ZrO_2	1300 °C, 16 h	I ≫ ZrO_2						
18	4% ZrO_2	1300 °C, 16 h	I ≫ ZrO_2			4.997	13.912	160 – 180[h]	None < 670[h]
19	2% MgO	1000 °C, 16 h	M >>> V_3O_5	4.958	13.945				
20	4% MgO	1000 °C, 16 h	M	4.959	13.948			20 – 80[g]	
21	6% MgO	1000 °C, 16 h	M >>> Spinel	4.958	13.986				
22	6% MgO	1350 °C, 16 h	M ≃ I >>> Spinel	4.960	13.967	4.998	13.891		
23	10% MgO	1000 °C, 16 h	M > Spinel						
24	10% MgO	1350 °C, 16 h	I ≫ Spinel						
25	16% Fe_2O_3	1350 °C, 16 h	M ≫ Fe_3O_4	4.975	13.959			< 121[h]	190–210[h,j]

[a] Analysis of metal ion impurity by emission spectrographic techniques. Values are χ in $(V_{1-x}Ti_x)_2O_3$ or $(V_{1-x}Zr_x)_2O_{3+2x}$.
[b] In ceramic samples the mole% dopant was taken as the starting ratio.
[c] Samples 1–13 grown in KF median by reaction of V_2O_3 + VN in argon atmosphere. Dopant added to melt as listed.
[d] Samples 14–25 fired in Pt boat under argon (No. 25-under nitrogen).
[e] M-metal, I-insulator. In multiphase samples, proportions indicated by >, <, and ≈. Estimates were made from x-ray powder patterns.
[f] Parameters determined either from Guinier or Debye–Scherrer powder patterns and accuracy is ≈0.02%.
[g] Determined from resistivity and/or magnetic susceptibility measurements.
[h] Approximate range observed in x-ray diffraction measurements.
[i] Only I observed at 373 °K but only ≈80% conversion to M before 150 °K.
[j] In 16-mole% Fe_2O_3 samples there is M → I transition on cooling which is opposite to other dopants. At the transition—a: 4.968 → 4.997 Å, c: 13.972 → 13.924 Å, giving $\Delta V/V \approx 0.8\%$.

TABLE II. Comparison of lattice parameters in monoclinic phase.

Sample	a(Å)	b(Å)	c(Å)	β^0
$x=0.00$	7.255(3)	5.002(2)	5.548(2)	96.75(2)
0.038 Cr	7.277(7)	4.997(5)	5.540(5)	96.74(5)
0.01 Al	7.272(2)	5.002(2)	5.538(2)	96.73(2)
4-mole% ZrO_2	7.278(2)	5.003(2)	5.532(2)	96.70(2)
20-mole% TiO_2	7.292(3)	5.001(2)	5.536(2)	96.76(2)

mixture before pressing it into a pellet for subsequent heat treatment. As discussed below, the temperature at which the samples are made has a marked effect on the properties of the product.

The different samples are characterized in terms of their position relative to pure V_2O_3 in the generalized phase diagram shown in Fig. 1. Powder x-ray diffraction measurements at room temperature are used to detect a discontinuous change in lattice parameters which would indicate a M-I transition as a function of doping with a particular ion. These results are summarized in Table I and Fig. 2. Powder x-ray measurements were made on some samples as a function of temperature using a Phillips diffractometer and either a platinum-strip heater or a temperature-controlled stream of nitrogen gas. Some of the results are shown in Fig. 3. The temperature range covered was 120–650 °K. One or more of the M-I, M-AF, and I-AF transitions were detected in several samples and the observed transition temperatures are reported in Table I. The lattice parameters for several samples in the AF phase are compared in Table II. In addition, the coefficients of thermal expansion in the M and I phases were determined during the course of this work and they are listed in Table III.

The phase diagrams for different dopants and the character of the different phases can also be checked independently by magnetic susceptibility and resistivity measurements as a function of temperature. These measurements were made as described in Refs. 2 and 7 and typical results for the M-AF transition in the $(V_{1-x}Ti_x)_2O_3$ system are shown in Fig. 4. The high-temperature susceptibility of samples, some of which exhibit and some of which do not exhibit a M-I transition, are compared to that of pure V_2O_3 in Fig. 5. Similar results for the electrical resistivity as a function of temperature are plotted in Fig. 6. The generalized phase diagram (Fig. 1) shows that pressure tends to make all samples more metallic. Resistivity measurements versus temperature and pressure were made for both Ti- and Zr-doped samples in the apparatus described earlier.[2]

The results for a sample with $x=0.038$ Ti and $x=0.003$ Zr are shown in Figs. 7 and 8, respectively. The critical pressure for the appearance of the AF phase with decreasing pressure at 4.2 °K was determined by measuring the resistivity; some results are shown in Fig. 9. The critical

TABLE III. Coefficients of thermal expansion at 298 °K.

Sample No.	$\frac{1}{a}\left(\frac{da}{dT}\right)\times 10^6$ °K^{-1}	$\frac{1}{c}\left(\frac{dc}{dT}\right)\times 10^6$ °K^{-1}
	Metallic phase	
$x=0.00$	20.2 ± 0.3	−8.6 ± 0.3
0.04 Ti	20.4	−5.6
4-mole% MgO	25.5 ± 2.0	−9.5 ± 2.0
16-mole% Fe_2O_3	15.0 ± 1.0	−4.4 ± 2.0
	Insulating phase	
0.038 Cr	8.8 ± 1.0	3.5 ± 1.0
4-mole% ZrO_2	8.8 ± 1.0	3.5 ± 1.0
4-mole% ZrO_2	11.3 ± 2.0	≈0 ± 2

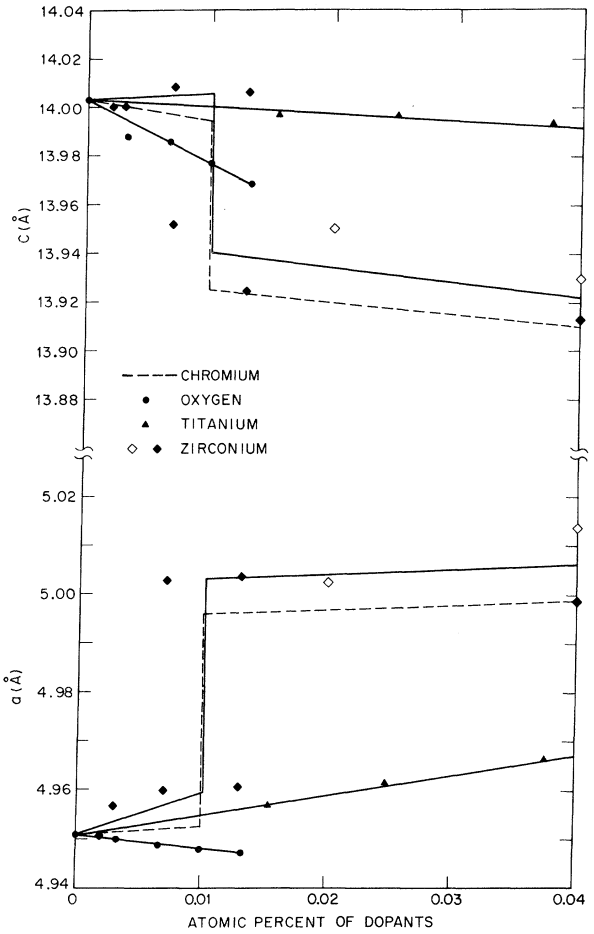

FIG. 2. Lattice parameters of $(V_{1-x}M_x)_2O_3$ vs x for different dopants M at room temperature. The closed symbols are this work; open symbols, Ref. 8. The dashed curve is for M = Cr after Ref. 2.

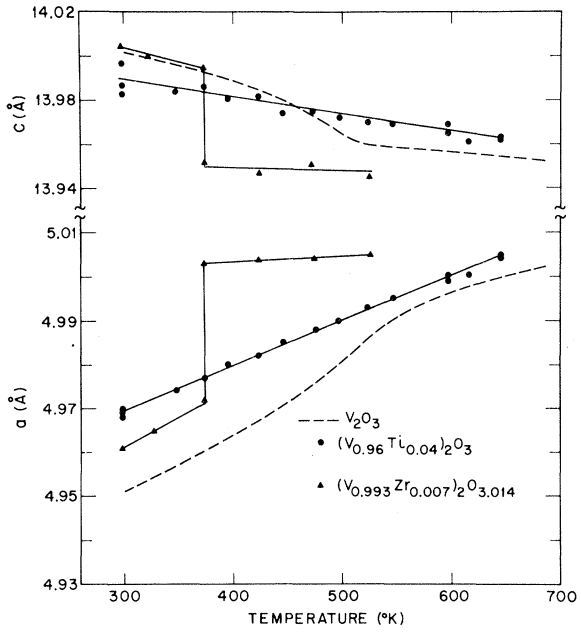

FIG. 3. Lattice parameters vs temperature for samples of doped V_2O_3 showing the M-I transition in a Zr-doped sample and the absence of a high-temperature anomaly in a Ti doped sample. The dashed curves are for pure V_2O_3 after Ref. 2.

pressures observed in both the Ti- and Cr-doped systems are summarized in Fig. 10.

III. PROPERTIES OF DOPED SAMPLES

A. Titanium

MacMillan made ceramic samples by firing mixtures of V_2O_5 and Ti_2O_3 in hydrogen.[8] His measurements of the resistivity as a function of temperature showed essentially no change in the M-AF transition temperature but a large decrease in the resistivity of the AF phase. In a recent preliminary report it was shown that the M-AF transition temperature decreased rapidly with increasing Ti content in our crystals shown by the appropriate open and closed circles in Fig. 1.[3] This is clearly seen in the magnetic-susceptibility measurements shown in Fig. 4 and the transition temperatures are given in Table I. According to Fig. 1, if the addition of Ti moves a sample to the more metallic side then the anomalies observed in the physical properties of pure V_2O_3 in the 500–600 °K range should be absent. The lattice parameter (Fig. 3), magnetic susceptibility (Fig. 5), and electrical resistivity (Fig. 6) measurements show a smooth variation through this region, in contrast to V_2O_3.

Previous studies established a three-dimensional phase diagram for the $(V_{1-x}Cr_x)_2O_3$ system[2] and presented data showing the suppression of the AF phase in the $(V_{1-x}Ti_x)_2O_3$ system.[3] Coupled with the data given above, the three-dimensional diagram can be extended. In Figs. 9 and 10 the critical pressure for the M-AF transition with decreasing pressure is 19.5 kbar for V_2O_3. It should be noted that P_c is lower in crystals grown by our technique than was found earlier for the crystals grown by flame fusion (23 kbar).[9] This is in agreement with the difference in $T_{M\text{-}AF}$ at 1 atm for the two different materials—150 and 164 °K. In other words the zero of pressure in Fig. 1 moves to the right or left as the stoichiometry changes but the over-all shape of the phase boundary remains essentially constant. The variation of $T_{M\text{-}AF}$ at 1 atm for the Ti-V-Cr sesquioxides is shown in Fig. 1 along with the scaled pressure experiments. The different critical pressures at 4.2 °K are shown in Fig. 10. As this is a first-order transition, there is a 2–3 kbar hysteresis observed between the transition with increasing and with decreasing pressure (see Fig. 7, for example). Part of this hysteresis is probably experimental in origin and results from friction in the high-pressure apparatus. The true thermodynamic-equilibrium–transition pressure is

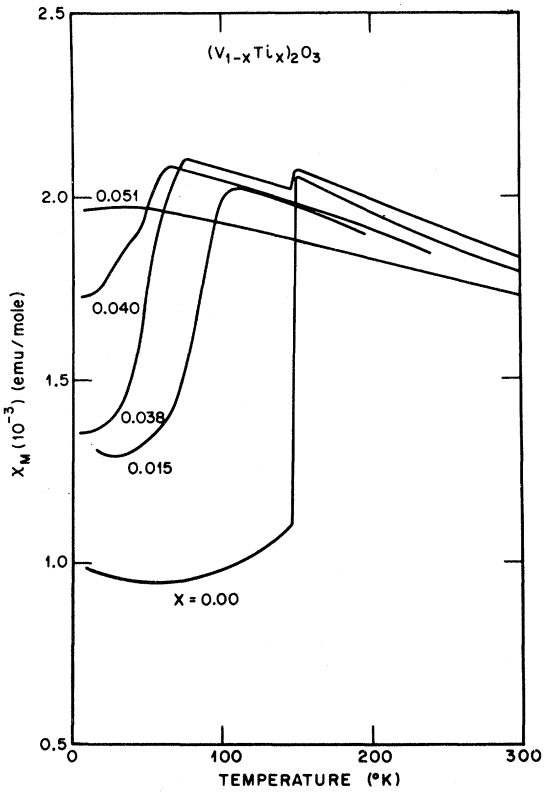

FIG. 4. Magnetic susceptibility vs temperature for several samples in the $(V_{1-x}Ti_x)_2O_3$ system. The curves show the suppression of the metal-antiferromagnetic-insulator transition temperature with the addition of Ti. The small drop in χ in the sample $x = 0.038$ at 150 °K is probably due to a second phase.

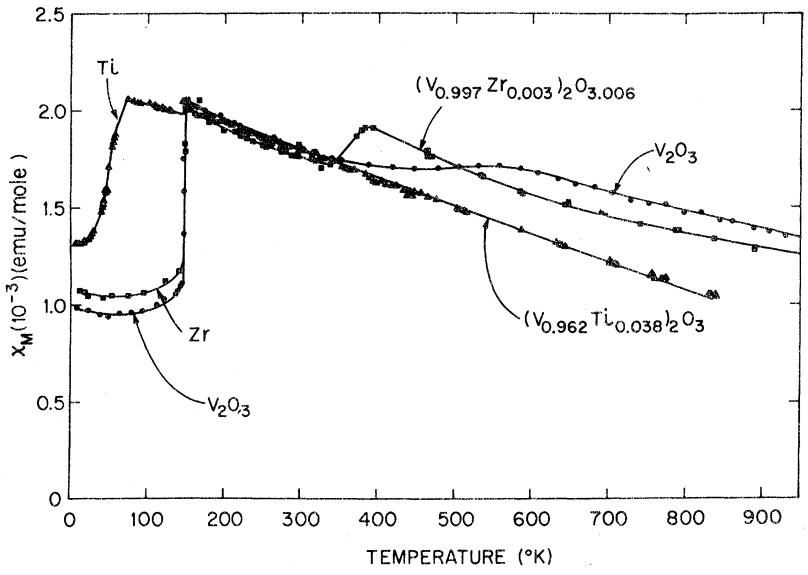

FIG. 5. Magnetic susceptibility vs temperature for samples of doped V_2O_3 showing the M-I transition in a Zr-doped sample and the absence in a high-temperature anomaly in a Ti-doped sample.

somewhere in the hysteresis loop. Within experimental error there is a linear variation of critical pressure with composition. The experimental errors are fairly large, as shown by the scatter of the points, so that some curvature or a small change in slope at pure V_2O_3 is not ruled out. There are errors arising from the quasihydrostatic nature of the experiment and this is illustrated in Fig. 10 where the observed P_c is dependent on the orientation of the crystal in the high pressure apparatus. In addition, the pressure calibration is based on an assumed linear relation between true pressure and applied load which is scaled to the transition in Bi at 25.4 kbar. This assumption is open to question at low pressures and in fact the M-I transition observed in the Cr sample with $x=0.019$ is 1.5 kbar higher than that previously observed in the piston cylinder apparatus.[10]

Combining the earlier data and that shown in Figs. 1 and 10 leads to the three-dimensional phase diagram shown in Fig. 11. The AF phase closes out smoothly as one moves from Cr to Ti doping.

The behavior of the Ti-doped single crystals is markedly different from that reported by MacMillan.[8] In growing the crystals it is assumed that the reaction mixture is sufficiently reducing so that Ti^{3+} is formed and goes into the lattice substitutionally. However, both Ti and V can exist as 3+ or 4+ ions as evidenced by the existence of both the sesquioxides and the dioxides. It is difficult to prove how the Ti goes into the lattice or how it is compensated. Chemically, Ti^{4+} is more stable than Ti^{3+}, and as shown below the addition of Zr^{4+} has a markedly different effect on V_2O_3 than the addition of titanium to the crystals. It is known that excess oxygen, like the addition of Ti

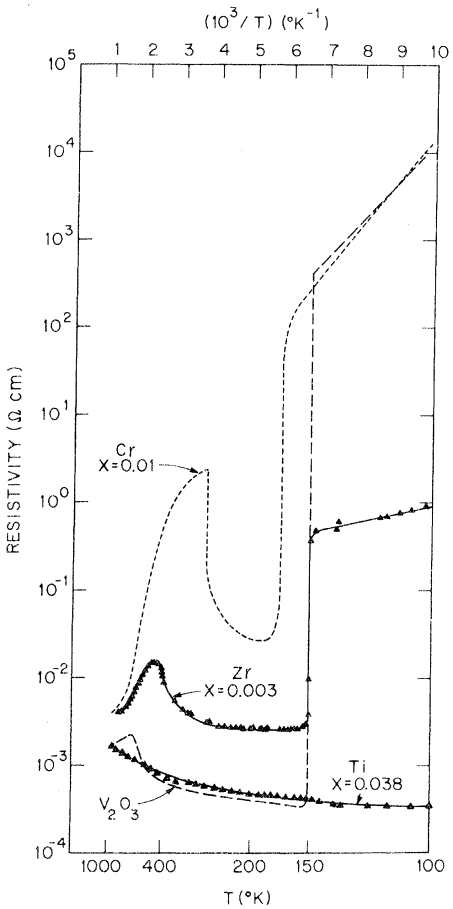

FIG. 6. Comparison of the electrical resistivity perpendicular to the c axis vs temperature for doped samples of V_2O_3. The dashed lines for V_2O_3 and the Cr-doped sample are from Ref. 2. Note presence or absence of high-temperature transition as in Figs. 3 and 5 and the low resistivity in the AF phase of the Zr-doped sample.

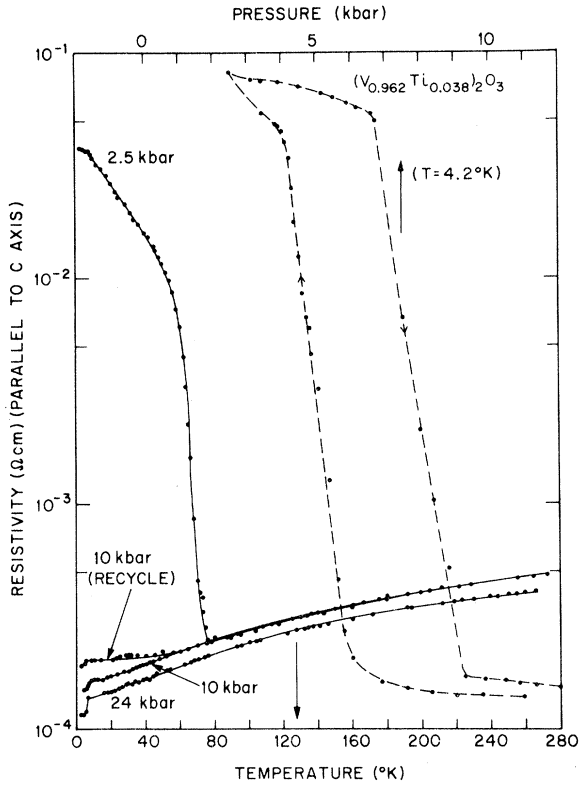

FIG. 7. Electrical resistivity parallel to the c axis vs temperature for $(V_{0.962}Ti_{0.030})_2O_3$ at several pressures showing the suppression of AF phase. Note deterioration of sample after cycling through the M-AF transition. Dashed curves are the resistivity at 4.2 °K vs pressure (upper scale) showing the hysteresis in the M-AF transition.

to the crystals, suppresses the M-AF transition. Therefore, it is reasonable to assume that if the addition of TiO_2 to V_2O_3 results in an M-I transition, then the Ti^{4+} ion is responsible. Ceramic samples were made from different mixtures of V_2O_3 and TiO_2. The x-ray studies at room temperatures reveal a discontinuous expansion of the lattice with increasing TiO_2 content similar to that found for the addition of Cr. X-ray measurements as a function of temperature in a sample of 20-mole% TiO_2 and 80-mole% V_2O_3 still show a M-AF transition in the range 150–160 °K similar to pure V_2O_3 and a transition to the I phase somewhere below 373 °K. This strongly suggests that the addition of Ti^{3+} stabilizes the M phase but that the addition of Ti^{4+} stabilizes the I phase. The present measurements suggest that the absence of any large change in the M-AF transition temperature in MacMillan's samples may have resulted from the presence of Ti^{4+} instead of Ti^{3+}.

The addition of TiO_2 to V_2O_3 is limited. A phase isostructural to V_3O_5 has been reported for the appropriate mixture of TiO_2 and V_2O_3.[11] Above the limit of solubility a two-phase region will exist and the x-ray patterns of the 20-mole% TiO_2 sample show both a corundum and a V_3O_5 phase. A detailed study was not made but the solubility limit appears to be between 10- and 20-mole% TiO_2.

B. Zirconium

Titanium can exist both as a 3+ and a 4+ ion. In order to establish more clearly the effect of a 4+ ion on V_2O_3 some samples containing Zr^{4+} were made. Zr^{4+} is very stable and it is unlikely that the ZrO_2 is reduced in the reaction mixture. Single-crystal samples do show a shift to the insulating side as shown in the x-ray (Fig. 3), magnetic-susceptibility (Fig. 5), and resistivity (Fig. 6) measurements. In all cases a temperature induced M-I transition is observed in addition to the M-AF transition. Unlike the results for the addition of Cr or excess oxygen, the resistivity in the AF phase is drastically reduced relative to that in pure V_2O_3 (Fig. 6) due to a decrease in the activation energy. The M-AF transition temperature is es-

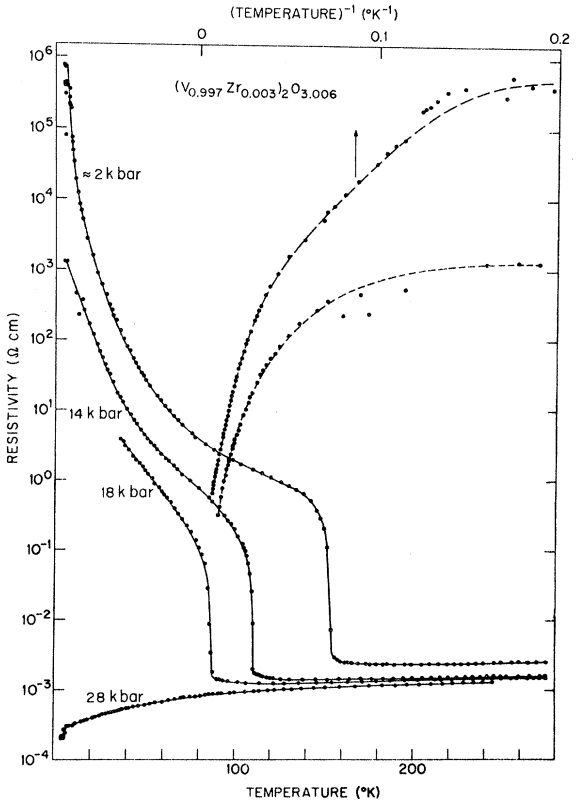

FIG. 8. Electrical resistivity perpendicular to the c axis vs temperature for $(V_{0.997}Zr_{0.003})_2O_{3.006}$ at several pressures showing the suppression of the AF phase. The resistivity vs reciprocal temperature (upper scale) is shown for the two lowest pressures. The anomaly at low temperatures in the 28-kbar curve may be due to the presence of superconducting VN as discussed in the text.

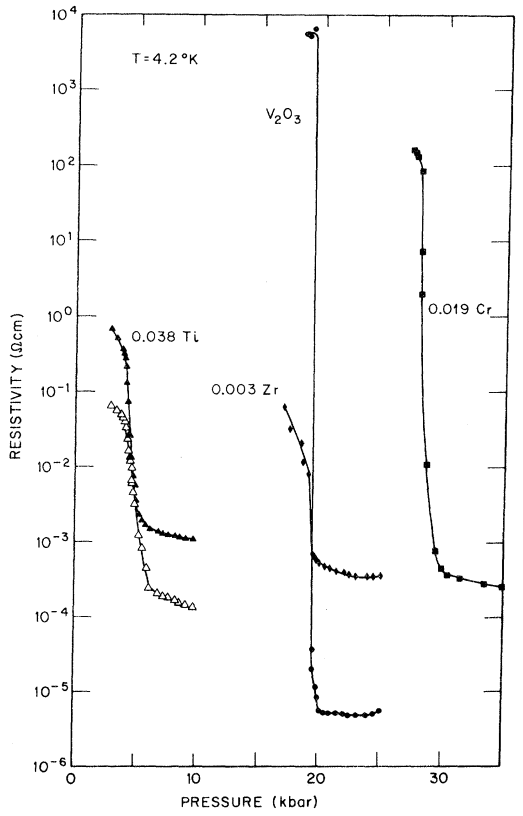

FIG. 9. Electrical resistivity perpendicular to the c axis (closed symbols) vs pressure at 4.2 °K for doped V_2O_3. All curves are for decreasing pressure, the curve for Ti (open triangles) is from Fig. 7. The two Ti curves are from two crystals mounted in the high-pressure apparatus together but with different orientation thus showing deviations from true hydrostatic conditions in the experiment.

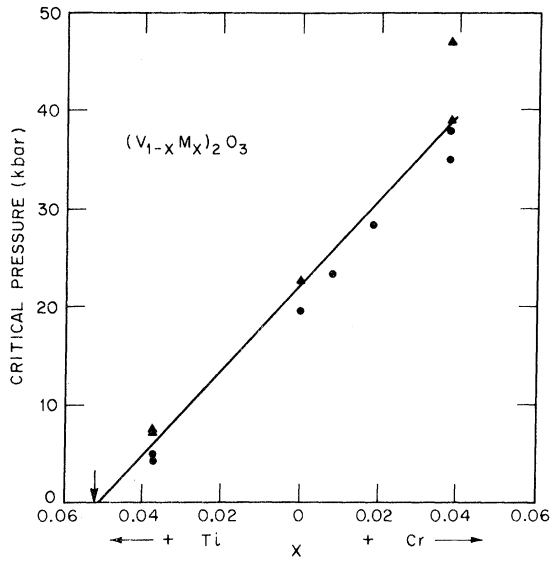

FIG. 10. Critical pressure at 4.2 °K for the M-AF transition plotted vs the concentration of Ti or Cr in V_2O_3. Triangles and circles are for increasing and decreasing pressure, respectively.

sentially unchanged similar to the samples containing Ti^{4+}. In agreement with the idea of a common P-T phase diagram, the critical pressure for the Zr doped samples is also similar to that of pure V_2O_3 (Fig. 9). It is interesting to note that the Zr-doped resistivity data indicate some evidence for a collapsing gap in the insulating phase. This effect can be seen both in the temperature dependence of resistivity and the fact that the discontinuity at the critical pressure becomes smaller as the temperature is lowered (Fig. 8). Such an effect is not seen in pure V_2O_3.

The resistivity of the metallic phase above the critical pressure has an anomaly at low temperatures as shown in Figs. 8 and 12. This break was observed in all three curves taken in the metallic phase. Since all the crystals are grown under similar conditions, a sample of pure V_2O_3 and one with $x = 0.003$ Zr were run together in the high-pressure apparatus. A warming curve was recorded at 29 kbar (Fig. 12). The 28-kbar curve from the previous high-pressure experiment is also shown in addition to curves from the Ti experiment and a Cr experiment described in Sec. IV. As can be seen, pure V_2O_3 does not exhibit an anomaly at low temperatures whereas both the Zr and Ti samples do. The temperature of the anomalies is similar to the superconducting transition temperature of VN (7.5 °K)[12] which is known to be a trace occluded second phase. The magnetic susceptibility of many of our single-crystal sam-

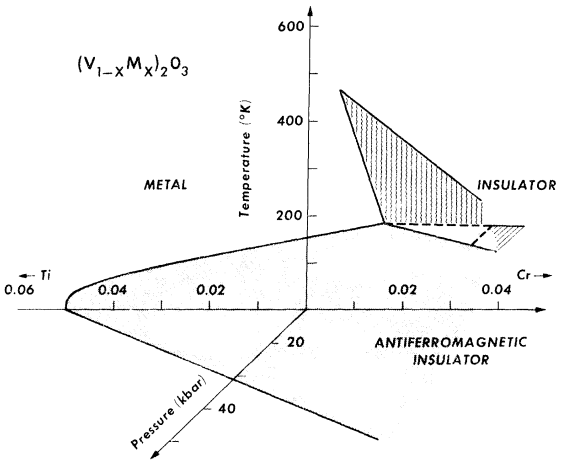

FIG. 11. Temperature-pressure–composition phase diagram showing M-I, M-AF, and I-AF surfaces. M-I surface terminates at a solid-solid critical line after Ref. 10.

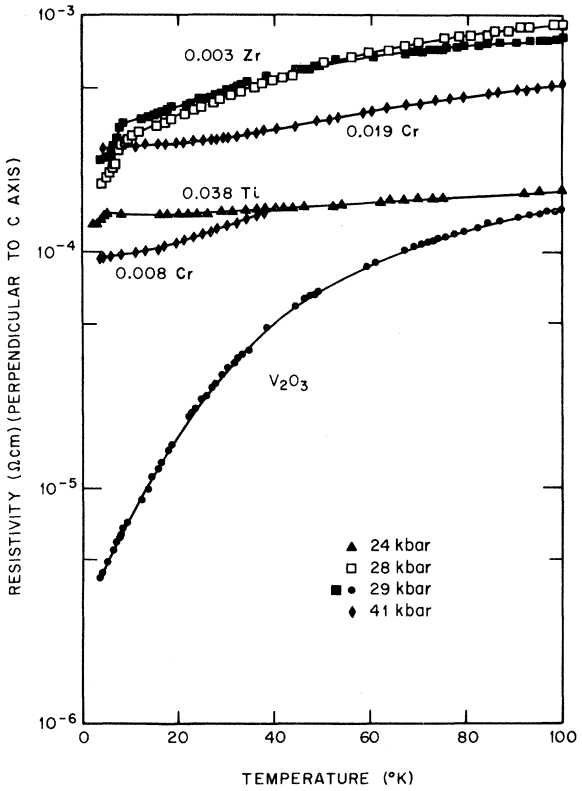

FIG. 12. Electrical resistivity perpendicular to the c axis vs temperature for samples of doped V_2O_3 obtained in the metallic phase above the critical pressure for suppression of the AF phase. Note the large increase in the residual resistivity with doping. The reproducibility of the experiment is shown by the two curves for Zr samples from different experiments (open and closed squares).

ples show a diamagnetic shift near 7 °K which is indicative of a superconducting transition. This suggests that the anomalies result from occluded VN and are not intrinsic properties of the doped crystals. Further experiments are needed as the pure V_2O_3 and Cr-doped crystals do not exhibit the phenomena (see Fig. 12).

The results on ceramic samples are similar to the single-crystal samples and show a shift to the insulating side of V_2O_3 in the generalized phase diagram. In making the ceramic samples of Zr-doped V_2O_3, a reaction temperature of 1300 °C resulted in a change to the I phase with only a small residual to ZrO_2. However, the work of Foex[13] and also that of MacMillan[8] shows that V_2O_3 becomes deficient in oxygen at temperatures much above 1000 °C. It is not known whether this is also true of the Zr-doped ceramic samples.

C. Magnesium and Iron

It appears from the experiments reported in Secs. III A and III B that 4+ ions such as Ti^{4+} and Zr^{4+} stabilize the insulating phase. A few experiments were done on the addition of a 2+ ion in the form of Mg^{2+}, but the results were not conclusive. MacMillan made ceramic samples by firing V_2O_5 and 2- and 4-mole% MgO at 1360 °C under hydrogen.[8] His magnetic-susceptibility measurements on these samples show a sharp reduction in the M-AF transition temperature which suggests a metallic shift. Our ceramic samples which were prepared at 1000 °C also show a reduction of $T_{M\text{-}AF}$ (Table I) and coefficients of thermal expansion (Table III) which are compatible with the other metallic phases. With increasing percentages of MgO a small amount of a spinel phase (probably MgV_2O_4) appeared, indicating limited solubility of Mg in V_2O_3 at this reaction temperature. Ceramic samples (6–10-mole% MgO) made at higher temperatures showed less of the second-spinel phase but an expanded-corundum or insulator phase was present. It seems reasonable that at the higher temperatures more Mg should be soluble in V_2O_3 and that the resulting sample would be more oxygen deficient. The observed differences in samples suggests that both the cation dopant and the oxygen stoichiometry influence the metallic and insulating properties of V_2O_3 and that much more detailed experiments will be required to determine the chemical nature of the different impurity centers.

A discontinuity in the lattice parameters in the $(V_{1-x}Fe_x)_2O_3$ system was observed at $x = 0.16$ by Cox, Takei, Miller, and Shirane.[14] This would suggest an insulating shift and recent Mössbauer studies by Wertheim, Remeika, Guggenheim, and Buchanan confirm the nature of the transition.[15] X-ray diffraction measurements on one of their samples with $x = 0.16$ show that there is a temperature-induced transition (Table I). However, in contrast to the Cr-, Al-, or Zr-doped samples, the collapsed-corundum or metallic phase is stable above the transition for Fe instead of below as with the others. This shows that the slope of the phase boundary in a T-P phase diagram has the opposite sign. Note that in a T-V phase diagram the metallic phase is always the high-temperature phase even in $(V_{0.96}Cr_{0.04})_2O_3$.[2] Finally, another difference in the iron system is that the transition occurs at a much higher concentration, namely, $x \approx 0.16$ instead of $x < 0.02$ for the other dopants. The transition is still a sharp function of concentration and temperature, which argues against giant cluster being responsible for the transition.

IV. DISCUSSION OF DOPING EXPERIMENTS

Considerably more work must be done before firm theoretical conclusions can be drawn about the effect of the various dopants on the electronic structure of V_2O_3. We shall separate the discussion of the various dopants according to valence,

since it appears that this rather than ionic size is the controlling factor. In the case of the Ti^{4+} and Zr^{4+} it is not clear how they enter the lattice. It is possible that the 4+ ions enter the lattice in such a way as to create random-rutile–type crystallographic shear planes similar to the corundum shear planes observed in the Magnéli phases.[16,17] These planes would allow the 4+ ion to be compensated locally and may represent planes that hinder metallic conduction, thus driving the system more insulating. Random-rutile shear planes offer an attractive alternative to having V vacancies in the experiments mixing TiO_2 and V_2O_3. If such shear planes existed in metallic V_2O_{3+x} one must assume that the VO_2 planes are metallic, whereas TiO_2 and ZrO_2 are insulating.

In those cases in which the ion is believed to be 3+, it is reasonable to assume they enter the lattice substitutionally. Some evidence that Fe^{3+} enters substitutionally can be obtained from the fact that the Mössbauer data[15] show no structure that can be attributed to local differences in environment. Assuming that Cr^{3+} and Ti^{3+} enter substitutionally, one still can only speculate on the nature of their effect on the electronic structure of V_2O_3.

A number of models have been proposed for the electronic band structure of V_2O_3[18–20]; at this time we will limit our discussion to a few minimal statements that can be made. First, it is quite clear that there is a strong coupling of the electrons in the bonding orbitals between the c-axis pairs. In the isostructural compounds Ti_2O_3 and Cr_2O_3 the experimental evidence is clear. Bonding between the Ti^{3+} c-axis pairs gives a reasonable explanation of the metal-insulator transition in Ti_2O_3.[20] On the other hand, in Cr_2O_3, while it is clear from the magnitude of the moment that intra-atomic Hund's-rule coupling has broken down the bonding, there is a large residual interaction between the c-axis pairs. This shows up in the exchange interaction which is anomalously large for t_{2g} orbitals.[21] There is likely to be considerable cancellation between the interaction through the anions and direct cation overlap so that the magnitude of the total interaction will be a sensitive function of position. This sensitivity is seen in Cr^{3+} pairs where the nearest-neighbor exchange integral changes by a factor of 2 on going from Cr^{3+} pairs in Al_2O_3[22] to Cr_2O_3. Thus we conclude that in the paramagnetic state of V_2O_3 the band associated with the a^T (Goodenough[20]) bonding orbitals along the c axis will probably be lower in energy than the e^T bands which come from orbitals which lie in the plane. Second, judging from the soft-x-ray work of Fischer[23] the occupied d bands are several eV wide. The presence of the crossover transition from the oxygen $2p$ levels to the $I_{II,III}$ levels of the vanadium indicates a sizable covalent mixture of the d bands with the cation $2p$ orbitals. Band-structure calculations on the transition-metal oxides support the view that the $2p$-$3d$ covalent mixture leads to bandwidths several eV wide.[24] In the AF phase alternative models have the a^T bands either above[20] or below[18,19] the e^T bands. In the latter model the low value $(1.2\mu_B)$[25] of the ordered moment in the AF phase is caused by the trapping of one electron per V in a filled a^T band split off from the e^T bands. We believe that it is unlikely that bands several eV wide are crossing one another in a phase transition below room temperature as Goodenough[20] has suggested. We find it most reasonable to assume that a substantial overlap of the a^T and e^T bands is present at all temperatures in V_2O_3.

It is difficult on the present evidence to be very definite about the role of the a^T-e^T overlap at the transitions. The localized-to-itinerant transition that occurs in V_2O_3 is probably primarily in the e^T band which then induces localization in the a^T bands which becomes more complete as one goes from V_2O_3 to Cr_2O_3. This interpretation is consistent with the expansion in V-V distances in the plane and along the c axis when Cr is added. The relationship between the general ideas of the Mott transition and the detailed nature of the first-order transition in V_2O_3 and its alloys is not as yet understood.

The simplest explanation of the doping experiments then is that the Cr^{3+} ions are a localized impurity and that they delete a state from the e^T and a^T bands. It can be shown that deleting a state from an almost localized band is equivalent to a band narrowing. Since it is well known that the Mott transition depends on the ratio of the bandwidth to the intra-atomic Coulomb interaction, the band narrowing will cause a transition to the insulating phase.[26] Similar considerations would hold for Al^{3+} and Sc^{3+}. Likewise, Ti^{3+} adds a slightly larger e^T orbital to this band and therefore causes an increase in the bandwidth and a movement away from localization. This is consistent with the data but why such a mechanism leads to the smooth variation as one crosses through pure V_2O_3 at $x=0$ in Fig. 10 is not clear. Finally, assuming the major effect of Cr and Ti is on the bandwidth gives rise to a natural explanation of the scaling of pressure and doping since pressure undoubtedly increases the bandwidth.

It has been suggested[20] that the inhomogeneities and randomness introduced by the Cr^{3+} ions may be responsible for the metal-insulator transition observed at room temperature. This seems to us unlikely since the phase-diagram studies[1,2,10] show that the high-temperature anomaly in pure V_2O_3 is clearly associated with the phase transition induced by the Cr. For this reason we prefer

the explanation that the Cr^{3+} ions are acting essentially in a uniform fashion and induce a Mott transition[5,1] by narrowing the conduction band.

V. TRANSPORT MEASUREMENTS AT LOW TEMPERATURES

A. Residual Resistivity and T^2 Term

A large T^2 term was found in the electrical resistivity of the metallic phase at low temperature.[9] The original measurements were made on crystals grown by flame fusion, and they have been repeated using the crystals grown by our technique. The results of four different experiments are summarized in Fig. 13. The top curve is from the earlier work and the bottom curve is from the experiment discussed in Sec. III and is the same one shown in Fig. 12. In both these experiments the sample was surrounded by AgCl to provide a quasihydrostatic-pressure-transmitting medium. In the two experiments shown in the middle, the samples were placed in the girdle die in a miniature Teflon cell containing a mixture of n-pentane-isoamyl alcohol.[27] In this way, a truly hydrostatic pressure is applied at room temperature and then the pressure-transmitting medium freezes around the sample on cooling. The only nonhydrostatic stress results from the differential-thermal contraction on cooling. The leads were attached to the sample by evaporating four chromium-gold dots and soldering the leads to the dots using tin. The two middle curves were from completely independent experiments on different crystals from the same batch and show the over-all reproducibility of the experiment. The quality of the different crystals is markedly different and the resistivity ratios ($\rho_{298}/\rho_{4.2}$) for the curves are, from bottom to top, 65, 39, and 13. Fitting the middle curves below 25 °K with a straight line gives $\rho(\mu\Omega\,\mathrm{cm}) = 10 + 0.054T^2$. At higher temperatures, the temperature dependence decreases as seen in Fig. 12. In one of the hydrostatic experiments a warming curve was also taken at 24 kbar and the percent decrease in the coefficient of the T^2 term (B) per percent change in pressure was $d\ln B/d\ln P \sim 0.4$. In the earlier work on the crystal grown by flame fusion, the coefficient B decreased by a factor of 2 on doubling the pressure.[9]

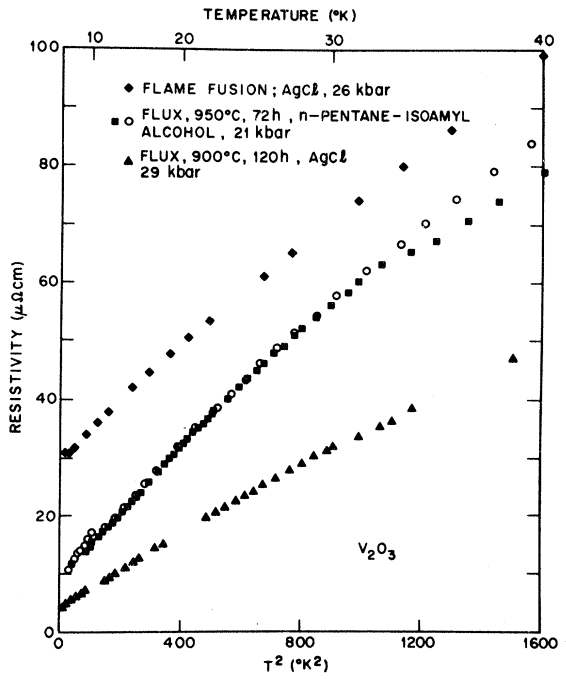

FIG. 13. Electrical resistivity vs T^2 for different samples of V_2O_3. The reproducibility of the experiment is shown for two separate experiments in the center (open circles and closed squares).

The residual resistivity ρ_0 of the different samples of "V_2O_3" varies over a factor of 6, and ρ_0 in doped samples (Fig. 12) varies over two orders of magnitude. It is clear that the residual resistivity is an extremely strong function of impurity content. In order to determine the concentration dependence of ρ_0, two Cr-doped samples with $x = 0.008$ and 0.019 [$(V_{1-x}Cr_x)_2O_3$] were run together in the high-pressure apparatus. The pressure was increased to 41 kbar at room temperature and then the resistivity measured on a warming cycle from 4.2 K [the samples were recooled to 4.2 K and ρ vs P measured to determine P_c (Figs. 9 and 10)]. Even at these concentrations the resistivity has a T^2 term at low temperatures with a coefficient similar to V_2O_3 as shown in Fig. 14.

The residual resistivities are plotted as a function of impurity concentration in Fig. 15. The point for $x = 0.038$ Cr is taken from the earlier studies. In that work a true four-probe measurement was not made, and an estimate of the correction for the contact resistance between the Pt contacts and the sample was made from an experiment on a Zr-doped sample where the correction was measured directly. Also included in Fig. 15 are points for $x = 0.038$ Ti and 0.003 Zr. The slope of ρ_0 vs Cr is 140 $\mu\Omega$ cm/at.% Cr. For Ti an average of points at $x = 0.038$ and 0.080 (Ref. 3) gives ~ 35 $\mu\Omega$ cm/at.% Ti. The point for Zr corresponds to 1000 $\mu\Omega$ cm/at.% Zr. These values are much larger than one finds for typical transition metals (~ 10 $\mu\Omega$ cm/at.%).[28]

B. Hall Coefficient

The Hall coefficient of V_2O_3 was measured at 20 kbar and helium temperatures in fields up to 9 kG. The nonmagnetic high-pressure die was the same as the one used in the nuclear-magnetic-resonance measurements on V_2O_3, and the calibra-

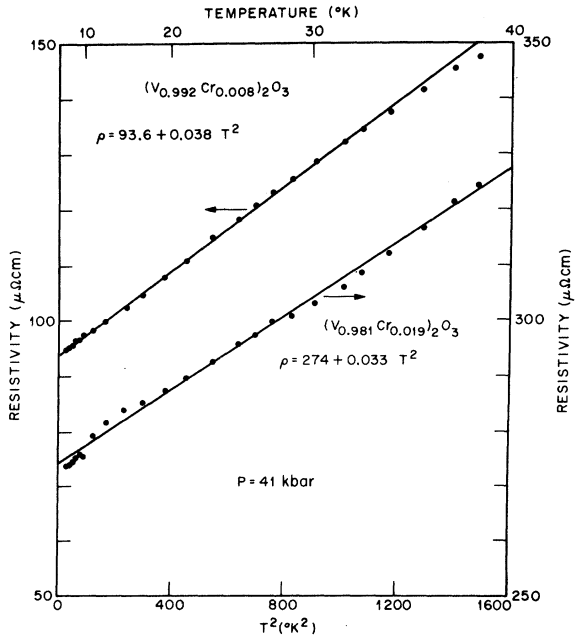

FIG. 14. Electrical resistivity vs T^2 for two Cr-doped samples. Curves show that T^2 term is unchanged but the residual resistivity increases rapidly on doping $x = 0.008$ Cr, left scale and $x = 0.019$ Cr, right scale. Both samples were run together at 41 kbar.

tion of the split-coil superconducting magnet was based on the ^{27}Al NMR frequency.[29] Two potential probes were attached to each side of the sample with silver paste and ultimately pressure contacts were made. Platinum-current leads covered the ends of the sample. Both dc and ac Hall measurements were made reversing the current and the field. Similar results for the Hall coefficient were obtained from both sets of probes and two entirely different preparations of crystals of V_2O_3. In the dc measurements a slight dependence of current results from sample heating. The average of all measurements gives $R_H = +(3.5 \pm 0.4) \times 10^{-4}$ cm^3/C. This value is only slightly larger than that reported for V_2O_3 at 150 °K and 1 atm, namely, $+2.4 \times 10^{-4}$ cm^3/C,[30–32] and this shows that the Hall coefficient is not a strong function of temperature and pressure.

VI. DISCUSSION OF TRANSPORT MEASUREMENTS

Several properties of the metallic state of V_2O_3, namely, the large values of the specific heat, the susceptibility, and the T^2 term in the resistivity have been shown to be consistent with a model of highly correlated electrons such as would be obtained if the e^T band of Sec. IV were assumed to be nearly localized.[3] In these circumstances each atom would exhibit localized spin fluctuations which give rise to the large values of the above properties. It has also been argued that although the number of low-energy spin excitations is large, the density of charge fluctuations is greatly suppressed[33] so that even though a Fermi surface exists the system will act very much like a semimetal. This statement has been verified by calculating the frequency-dependent conductivity in the pure metal via a Landau-type theory in which the parameters are obtained from the Gutzwiller approach to electronic correlation.[26] However, if one attempts to calculate the dc conductivity in the limit of weak scattering one finds that $\sigma = e^2 S_F L/12\pi^3$, where L is the mean free path and S_F is the Fermi-surface area. The mean free path L is proportional to the inverse of the concentration times the scattering cross section per impurity. If one assumes the cross section is not larger than the lattice constant squared then the residual resistivity per percent impurity would not be greater than ~ 10 $\mu\Omega$ cm, contrary to the experimental data in Fig. 14. It has been suggested[34] that the very large value of the residual resistivity in the Cr^{3+} samples can, however, be explained by assuming that an "insulating" cluster develops around each Cr^{3+} ion. The Cr^{3+} ion then acts resistively in a fashion similar to the giant magnetic-moment behavior of Fe in Pd.[35] In contrast to this, doping with Ti^{3+} would not lead to insulating clusters and the increase in residual resistivity is a factor of 4 less than that

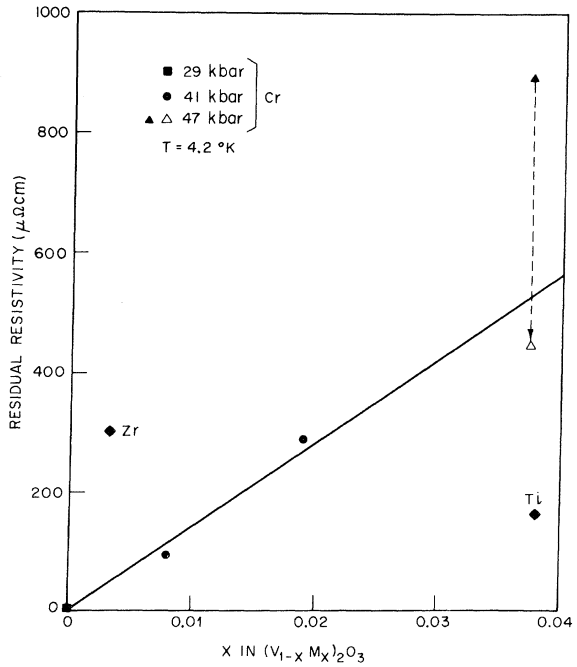

FIG. 15. Residual resistivity vs Cr concentration. The slope is 140 $\mu\Omega$ cm/at.% Cr. The point at $x = 0.038$ is discussed in the text. For comparison, points for Zr and Ti are included from Fig. 12.

found for Cr^{3+}.

If one takes the above view then the residual resistivity on doping with Cr^{3+} is consistent with the abovementioned model of the highly correlated metallic state of V_2O_3. The measurement of the Hall constant, however, is much more difficult to understand since at low temperatures the Hall constant can simply be related to the volume contained by the Fermi surface. One would then expect that above the characteristic spin-fluctuation temperature the Hall effect would be proportional to the inverse of the true number of charge carriers and therefore increase considerably.[26] The measurements indicate a small temperature dependence to the Hall constant so that this idea is not consistent with the data. Clearly, however, in a system as complicated as V_2O_3 the band structure is probably sufficiently complex that a proper interpretation of the Hall constant will have to await a better calculation.

It should be pointed out that the transport data are consistent with a model in which an s band or some other band crosses a localized band and causes a Kondo-type reduction of the localized moments. The localized moments could give the large susceptibility and specific heat and the T^2 resistivity due to their scattering of the conducting electrons.[36] Such a model appears to us to be quite unlikely since the d bands themselves are not expected to be narrow in V_2O_3 and the 4s bands of the V are probably a few eV above the occupied t_{2g} band. The latter statement is inferred from the optical data on Al_2O_3 which places the oxygen-2p-to-Al-3s transition edge at 10 eV while the separation between the oxygen-2p band and the occupied 3d band as measured by soft-x-ray emission in V_2O_3 is 6 eV. One does not expect the 4s band to move down appreciably in V_2O_3 since there is not a large difference in lattice constants.

In conclusion then we feel that a localized-to-nonlocalized (i.e., Mott) transition primarily within the e^T band is still the best available model for V_2O_3.

ACKNOWLEDGMENTS

We thank A. S. Cooper, E. Kelly, A. L. Stevens, and J. V. Waszczak for technical assistance.

*Present address: Brown-Boveri Research Center, CH-5401, Baden, Switzerland.

[1]D. B. McWhan, T. M. Rice, and J. P. Remeika, Phys. Rev. Lett. **23,** 1384 (1969).

[2]D. B. McWhan and J. P. Remeika, Phys. Rev. B **2,** 3734 (1970), and references therein.

[3]D. B. McWhan, J. P. Remeika, T. M. Rice, W. F. Brinkman, J. P. Maita, and A. Menth, Phys. Rev. Lett. **27,** 941 (1971).

[4]T. M. Rice and D. B. McWhan, IBM J. Res. Dev. **14,** 251 (1970).

[5]N. F. Mott, Proc. Phys. Soc. Lond. **62,** 416 (1949); Philos. Mag. **6,** 287 (1961).

[6]N. F. Mott, J. Phys. (Paris) 32, C1-11 (1971).

[7]D. B. McWhan, A. Menth, and J. P. Remeika, J. Phys. (Paris) **32,** C1-1079 (1971).

[8]A. J. MacMillan, Laboratory for Insulation Research, MIT Report No. 172, 1960 (unpublished).

[9]D. B. McWhan and T. M. Rice, Phys. Rev. Lett. **22,** 887 (1969).

[10]A. Jayaraman, D. B. McWhan, J. P. Remeika, and P. D. Dernier, Phys. Rev. B **2,** 3751 (1970).

[11]A. Magneli, L. Westman, B. Holmberg, L. Kihlborg, L. Asbrink, C. Nordmark, S. Anderson, and B. O. Marinder, Final Technical Report No. 1, [DA-91-591-EUC-B13], 1960 (unpublished)

[12]B. T. Matthias and J. K. Hulm, Phys. Rev. **87,** 799 (1952).

[13]M. Foex, J. Rech. Cent. Natl. Rech. Sci. **21,** 237 (1951).

[14]D. E. Cox, V. J. Takei, R. C. Miller, and G. Shirane, J. Phys. Chem. Solids **23,** 863 (1962).

[15]G. K. Wertheim, J.P. Remeika, H.J. Guggenheim, and D. N. E. Buchanan, Phys. Rev. Lett. **24,** 25 (1970).

[16]S. Anderson and J. Galy, J. Solid State Chem. **1,** 576 (1970).

[17]L. A. Bursill, B. G. Hyde, 0. Terasaki, and D. Watanabe, Philos. Mag. **20,** 347 (1969).

[18]N. F. Mott and Z. Zinamon, Rep. Prog. Phys. **33,** 881 (1970).

[19]M. Weger (unpublished).

[20]J. B. Goodenough, in *Progress in Solid State Chemistry,* edited by H. Reiss (Pergamon, New York, 1971), Vol. 5, p. 145.

[21]E. J. Samuelsen, M. I. Hutchings, and G. Shirane, Solid State Commun. **7,** 1043 (1969); Physica (Utr.) **48,** 13 (1970).

[22]L. F. Mollenauer and A. L. Schawlow, Phys. Rev. **168,** 309 (1968).

[23]D. W. Fischer, J. Appl. Phys. **40,** 4151 (1969).

[24]L. F. Mattheiss, Phys. Rev. B **5,** 306 (1972).

[25]R. M. Moon, Phys. Rev. Lett. **25,** 527 (1970).

[26]T. M. Rice and W. F. Brinkman, Phys. Rev. B **5,** 4350 (1972).

[27]A. L. Stevens (unpublished).

[28]N. F. Mott and H. Jones, *The Theory of Metals and Alloys* (Clarendon, Oxford, England, 1936).

[29]A. C. Gossard, D. B. McWhan, and J.P. Remeika, Phys. Rev. B **2,** 3762 (1970).

[30]V. P. Zhuze, A. D. Andreev, and A. J. Shelykh, Fiz. Tverd. Tela **10,** 3674 (1968) [Sov. Phys.-Solid State **10,** 2914 (1969)].

[31]A. S. Barker, Jr. and H. C. Montgomery (private communication).

[32]I. G. Austin and C. E. Turner, Philos. Mag. **19,** 939 (1969).

[33]T. M. Rice and W. F. Brinkman, in *Critical Phenomena in Alloys, Magnets and Superconductors,* edited by R. E. Mills, E. Archer, and R. Jaffee (McGraw-Hill, New York, 1971), p. 593.

[34]J. Friedel and J. R. Schrieffer (private communication).

[35]G. G. Low and T. M. Holden, Proc. Phys. Soc. Lond. **89,** 119 (1966).

[36]Resistivities associated with the Kondo effect may increase with temperature, cf. J. Kondo, Phys. Rev. **169,** 457 (1968).

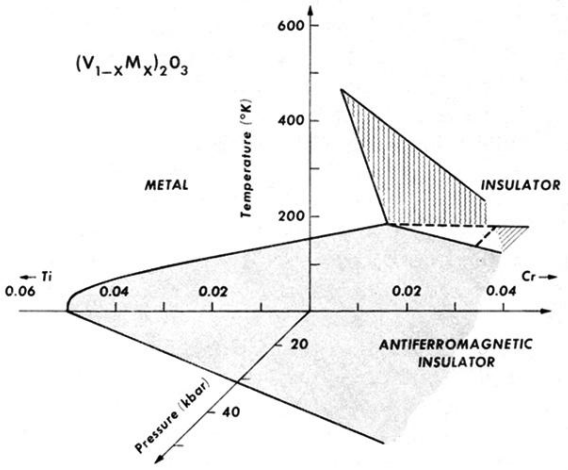

FIG. 11. Temperature-pressure–composition phase diagram showing M-I, M-AF, and I-AF surfaces. M-I surface terminates at a solid-solid critical line after Ref. 10.